JOURNAL OF CATALYSIS **110**, 275–284 (1988)

Support Effect on the Catalytic Activity and Properties of Sulfided Molybdenum Catalysts

H. SHIMADA, T. SATO, Y. YOSHIMURA, J. HIRAISHI, AND A. NISHIJIMA

National Chemical Laboratory for Industry, Yatabe Ibaraki, 305 Japan

Received June 1, 1987; revised November 5, 1987

The effect of the support on the catalytic activity and properties of molybdenum sulfide catalysts was investigated in order to obtain the fundamental information necessary for designing better hydrotreating catalysts. The catalytic activity for each catalyst was evaluated using model test reactions under high hydrogen pressure. The order of supports for hydrogenation (HYD) of 1-methylnaphthalene was $Al_2O_3 > TiO_2 > MgO > SiO_2$, while that for hydrocracking (HYC) of diphenylmethane and hydrodesulfurization (HDS) of dibenzothiophene was $TiO_2 > SiO_2 > Al_2O_3 > MgO$. Characterization of catalysts clarified that the catalytic activities depend on the structure and properties of the metal oxide which is the precursor of the active sulfide species. Formation of highly dispersed two-dimensional polymolybdate structures, which were observed on the Al_2O_3 and the TiO_2 supports, were the most favorable for high HYD activity. In contrast, the data indicate that the enhancement of HYC activity requires an electronegative form of the molybdenum species on which Brønsted acid sites can be formed under the reaction condition. HDS of DBT can be catalyzed on both kinds of active sites, although the product distribution is different.

INTRODUCTION

Sulfided molybdenum catalysts supported on γ–Al_2O_3 have long been used for hydrodesulfurization (HDS) of petroleum fractions. Recently, much attention has been paid to the application of molybdenum catalysts in coal liquefaction (*1*) or hydrotreating of petroleum residue. In these processes, several kinds of reactions besides HDS, such as demetallation, hydrodenitrogenation, or asphaltene conversion, need to be promoted on the catalyst. In order to obtain high levels of these catalytic activities, a proper combination of hydrogenation (HYD) and hydrocracking (HYC) activities is required as fundamental functions of the catalyst.

It is widely known that molybdenum sulfide catalysts have several different active sites where HYD, HDS, or HYC is catalyzed (*2–4*). A practical method for designing catalysts with favorable activity and selectivity is to find the support which best enhances the desired chemical properties of the catalyst.

Support effects on the catalytic activities of molybdenum catalysts have been studied by several researchers (*5–8*). Hattori *et al.* (*5*) investigated the reduction of NO_x over supported molybdate catalysts and indicated that the support affected the reduced form of molybdate, which was greatly related to the catalytic activity. Swanson *et al.* (*6*) studied support effects on the isomerization of hexane and reported that a weak interaction between Mo and the support resulted in highly reduced Mo which facilitates the isomerization. MuraliDhar *et al.* (*7*) and Massoth *et al.* (*8*) studied HDS, HYD, and HYC activities of supported molybdenum sulfide catalysts on various oxides under atmospheric pressure and stated that the catalyst support played an important role in the dispersion of molybdenum which was related to HDS and HYD activities of the catalyst. Differences observed for HYC activity were not attributed to the

0021-9517/88 $3.00

molybdenum sulfide catalyst itself, but to Brønsted acidity of the support.

The authors of the present paper reported on the strong effects the support has on HYC activity of sulfided molybdenum catalysts under high hydrogen pressure and suggested that strong support acidity is not necessarily required for HYC activity of the catalyst (*9*). Furthermore, high HYD and HDN activities for TiO_2-supported molybdenum sulfide catalysts were observed for hydrotreating of coal-derived liquids (*10, 11*).

As has been described above, catalytic activities of molybdenum catalysts are very dependent on the support used. As for the effect of the support on the catalytic properties, most of the investigations have pointed out the strong dependence of Mo dispersion upon the support properties. However, these features have not been studied under high hydrogen pressure where practical hydroprocessing is carried out. In particular, the correlation between HYC activity under high pressure and the properties of the sulfided molybdenum catalyst have not yet been clarified.

In the present paper, fundamental functions of molybdenum sulfide catalysts on several supports were evaluated using separate model reaction tests, such as HYC of diphenylmethane (DPM), HYD of 1-methylnaphthalene (1-MN), and HDS of dibenzothiophene (DBT). Besides the activity tests, several characterization techniques were used in order to obtain information about the structure and properties of the catalysts. Based on these experimental results, the correlation between the catalytic activity and the properties of the molybdenum catalysts will be discussed. Emphasis is placed on the HYC activity of the molybdenum sulfide catalyst under high hydrogen pressure.

METHODS

Catalyst Preparation

Four kinds of oxides were used as catalyst supports in this study. Commercially available supports were used for γ–Al_2O_3 (Catalysts and Chemicals Industry Co., Ltd.), SiO_2 (Davison grade 57), and MgO (Nakarai Chemicals Co., Ltd., reagent grade). The TiO_2 support was prepared by precipitation from an aqueous solution of $Ti(SO_4)_2$. The precipitation was carried out by adding the $Ti(SO_4)_2$ solution and $(NH_4)_2CO_3$ simultaneously to a vessel at a constant pH of 8.0. This was followed by heating (110°C for 1 h) and aging (room temperature for 24 h). The precipitate was subsequently washed until no SO_4^{2-} could be detected (using $BaCl_2$ solution). The resulting solid was dried for 19 h at 110°C and then calcined for 3 h at 500°C. All the supports were powdered and sieved to smaller than 1 mm before preparation of the catalysts. The surface area and pore volume values for each support were as follows: Al_2O_3, 170 m^2/g, 0.47 ml/g; TiO_2, 66 m^2/g, 0.17 ml/g; SiO_2, 266 m^2/g, 1.09 ml/g; MgO, 51 m^2/g, 0.16 ml/g.

A series of catalysts containing 10% of MoO_3 by weight was prepared by wet impregnation of each support with an aqueous ammonium paramolybdate solution. After drying for 19 h at 110°C, the samples were calcined for 3 h at 500°C.

Model Test Reactions

Hydrocracking (HYC) of diphenylmethane (DPM), hydrogenation (HYD) of 1-methylnaphthalene (1-MN), and hydrodesulfurization (HDS) of dibenzothiophene (DBT) were chosen as probe reactions for estimating the fundamental activities of each catalyst. All the model test reactions were carried out using 50 cm^3 autoclaves. The initial charge to the autoclave was 10 cm^3 of each reactant, 0.1 g of powdered catalyst, and 6.9 MPa of H_2. The catalyst was presulfided with 5% H_2S–95% H_2 gas for 1 h at 400°C before reaction. In the case of DBT, 20 wt% of dibenzothiophene/tetralin solution was used as a starting material. All the activity tests were performed at 400°C for 1 h. A gas chromatograph equipped with a crosslinked methylsilicone capillary column (Hewlett–Packard, Ultra No. 2, 50 m) was used in the analysis of the liquid product.

Characterization of the Catalysts

Temperature-programmed reduction (TPR) measurement. A 250-mg sample of each catalyst was reduced in a stream of H_2 (flow rate of 100 cm^3 min^{-1}) from 40 to 500°C at a rate of 10°C min^{-1}. Prior to each measurement the sample was preheated in a stream of N_2 at 500°C for 1 h to remove adsorbed water. The decrease in weight of the sample which was caused by reduction was detected by a microbalance (Shimadzu, TG-30).

Spectral measurements. X-ray photoelectron spectra were obtained using a Shimadzu ASIX-1000 spectrometer with $MgK_{\alpha 1,2}$ X-rays (270 W). All the samples were powdered and pressed into pellets, which were fixed on the holder using conducting paste to lower the charging effect. The binding energies, which were referenced to the gold (Au $4f_{7/2}$ = 83.8 eV) evaporated on the sample, were reproducible within ±0.1 eV.

Raman spectra were recorded on a JASCO R-800 spectrometer equipped with a double monochromator for oxide catalysts and a Spex Ramalog 4 triple monochromator for sulfided catalysts. The 514.5-nm line from an Ar^+ laser was used as the exciting source. The spectral shift width was 5 cm^{-1} and a laser power of ca. 50 mW at the sample was employed. The sample was pelletized and fixed to a holder, which was rotated to minimize sample heating. In the case of the sulfided catalysts, the sample was kept *in vacuo* during the measurement to avoid oxidation of the sample.

RESULTS AND DISCUSSION

Model Reaction Tests

The catalytic activities of the four differently supported Mo sulfide catalysts are summarized in Table 1. Hydrocracking of DPM over the molybdenum catalysts under the reaction conditions predominantly gave benzene and toluene. Small amounts of a hydrogenated compound (hexahydrodiphenylmethane) and polymerized compounds from toluene (methyldiphenylmethanes, etc.) were also obtained. HYC activities of the catalysts were evaluated based on the yields of benzene and toluene. Only 1- and 5-methyltetralins were produced during the hydrogenation of 1-MN. Biphenyl and cyclohexylbenzene were the main desulfurized products from DBT, while small amounts of tetrahydrodibenzothiophene were observed during the reaction. Yields of biphenyl and cyclohexylbenzene were used to calculate the HDS activity of the catalyst.

TABLE I

Support Effects on the Catalytic Activities of Sulfided Mo Catalysts

Support	HCK of DPM			HYD of 1-MN	HDS of DBT	
	Conv.[a] (%)	HCK[b] (%)	HYD[c] (%)	HYD[d] (%)	HDS[e] (%)	HBP/BP[f] (—)
Al_2O_3	2.9	2.0	0.9	20.3	17.1	0.80
TiO_2	28.1	27.3	0.5	11.8	26.9	0.85
SiO_2	6.5	5.3	1.1	0.8	19.7	1.02
MgO	0.0	0.0	0.0	3.3	4.7	0.67

[a] Total conversion.

[b] Yield of benzene and toluene.

[c] Yield of benzylcyclohexane.

[d] Yield of 1- and 5-methyltetralins.

[e] Yield of biphenyl and cyclohexylbenzene.

[f] Ratio of cyclohexylbenzene to biphenyl.

Among the oxides examined, the effectiveness order of the support for each activity was as follows,

HYC of DPM: $TiO_2 \gg SiO_2 > Al_2O_3 \gg MgO$

HYD of 1-MN: $Al_2O_3 > TiO_2 > MgO > SiO_2$

HDS of DBT: $TiO_2 > SiO_2 > Al_2O_3 > MgO$.

The most striking support effect was observed for HYC activity. The TiO_2-supported catalyst gave the highest HYC activ-

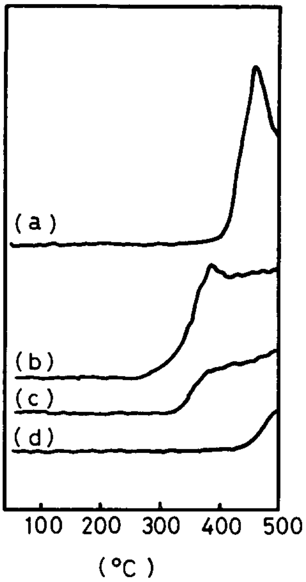

FIG. 1. TPR spectra for Mo oxide catalysts on various supports: (a) Mo/SiO_2, (b) Mo/TiO_2, (c) Mo/Al_2O_3, (d) Mo/MgO.

ity, while the MgO-supported one gave no conversion. The catalysts supported on Al_2O_3 and SiO_2 showed high selectivities for hydrogenated compounds. However, in spite of their high surface areas, neither gave high HYC activity. The order of the supports for HDS of DBT was the same as that for HYC of DPM, although the difference among the supports was smaller than that for HYC. For HYD of 1-MN, the Al_2O_3-supported catalyst gave the highest activity. The SiO_2-supported catalyst gave the lowest HYD activity, although in the HYC reaction of DPM and the HDS reaction of DBT it produced more hydrogenated products than the corresponding Al_2O_3. This result implies that HYC, HYD, and HDS active sites are not independent from each other and that HYC and HDS reactions affected the simultaneous HYD reaction.

Test reactions over the support alone were also carried out. No conversion of the starting materials was observed over any of the supports. All of the reactions were catalyzed to some extent over the molybdenum oxide catalyst on each support; however, this was much less than that of the sulfided catalysts. These results indicate that the active species were not unreduced Mo^{6+} nor double oxides which were reported to be acidic (*12*), but sulfided molybdenum species.

TPR. Figure 1 shows the TPR profiles of the calcined catalysts. The temperatures at which reduction of the catalysts began were as follows: TiO_2, 315°C; Al_2O_3, 325°C; SiO_2, 410°C; MgO, 460°C. The amount of hydrogen consumption (H_c) per molybdenum up to 500°C (H_c/Mo) was also dependent on the support: TiO_2, 1.3; SiO_2, 0.8; Al_2O_3, 0.5; MgO, 0.1. These results clearly indicated that the ease of reduction of molybdate depends on the support effect. Under the same conditions, pure MoO_3 powder showed little hydrogen consumption up to 500°C, suggesting that supported molybdate is reduced more easily than pure MoO_3 powder in the first stage (from Mo^{6+} to Mo^{4+}) below 500°C.

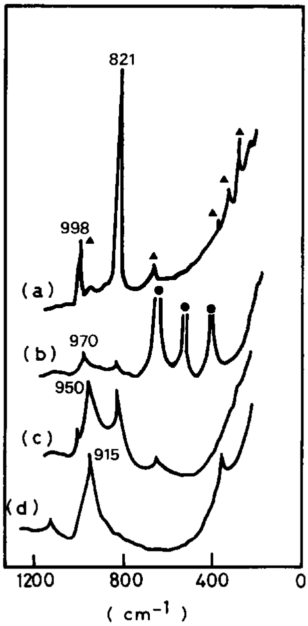

FIG. 2. Raman spectra for Mo oxide catalysts on various supports: (a) Mo/SiO_2, (b) Mo/TiO_2, (c) Mo/Al_2O_3, (d) Mo/MgO, (▲) from MoO_3, (●) from TiO_2.

Raman spectra. Figure 2 shows the Raman spectra for the calcined Mo catalysts. The SiO_2-supported catalyst gave many sharp bands which were in agreement with crystalline MoO_3. This indicates the formation of three-dimensional MoO_3 structures on the SiO_2 support. Taking into account that XRD showed no crystalline peak for the Mo/SiO_2 catalyst, the size of MoO_3-like crystalline structures must be smaller than a few nanometers.

For the Al_2O_3 and the TiO_2 supports, a broad band was observed between 900 and 1000 cm^{-1} in addition to the two crystalline bands (998 and 820 cm^{-1}). Brown *et al.* (*13*) assigned the broad and intense band to a Mo–O stretching vibration mode of the molybdate species. It was also indicated that the band originated from a two-dimensional polymeric surface molybdate species (*14, 15*).

Changes in the spectrum with Mo loading on the TiO_2 support are shown in Fig. 3. The upward shift of the broad band was observed with increasing Mo loading, and high levels of molybdenum loading resulted in the crystalline MoO_3 structure. The upward shift can be ascribed to the formation of more highly aggregated polymolybdate structures which form before monolayer coverage. After monolayer coverage the crystalline three-dimensional MoO_3 structure is formed. Figure 4 clearly indicates that the formation of two-dimensional polymolybdate levels out when the monolayer coverage was exceeded. These changes are similar to those observed on Al_2O_3 supports (*14–18*). The 4–6 Mo atom/nm^2 (when the monolayer coverage was reached) is close to that observed on Al_2O_3 (*19, 20*). A previous study (*21*) on the structure of supported molybdates using Raman spectroscopy also showed the similarity between the interaction of Mo on TiO_2 and that on Al_2O_3. Thus, the behavior of molybdate on TiO_2 is similar to that on Al_2O_3 and good dispersion can be achieved on both supports.

The MgO-supported catalyst showed no crystalline band for the molybdate, in spite of the fact that the surface area was smaller than that of TiO_2 or Al_2O_3 which exhibited crystalline bands. Comparison of the spectrum for the MgO-supported catalyst with the spectra for molybdenum anion solutions (*15*) implies that the 915-cm^{-1} band,

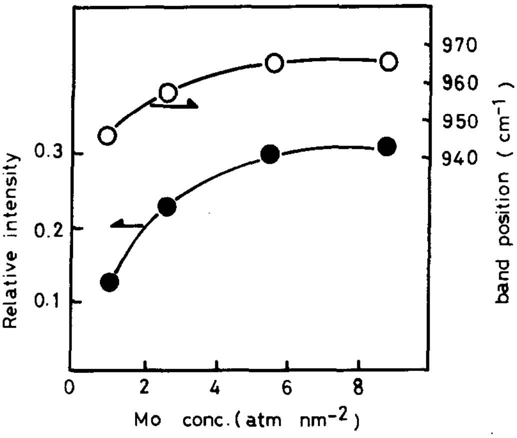

FIG. 4. Change in Mo–O stretching band intensity and band position with Mo loading on TiO_2 support. (Relative intensity is the band height ratio relative to the TiO_2 700-cm^{-1} band.)

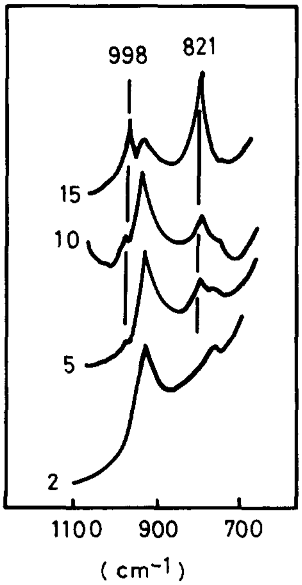

FIG. 3. Change in Raman spectra of Mo/TiO_2 oxide catalysts with Mo loading. (Numbers show the weight percent loading of MoO_3.)

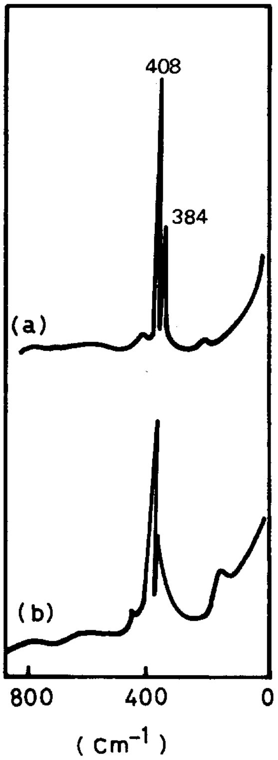

FIG. 5. Raman spectra for (a) crystalline MoS_2 and (b) sulfided Mo/Al_2O_3 catalyst.

which can be assigned to a Mo–O stretching vibration, is attributed to isolated molybdenum species. It is plausible that the molybdate was incorporated into the MgO matrix and formed a tetrahedral MoO_4^{2-} structure.

Figure 5 shows the Raman spectra for a MoS_2 powder and the sulfided Mo/Al_2O_3 catalyst. Two sharp bands (384 and 408 cm^{-1}) are characteristic for MoS_2 (*22*). Close correlation between the band positions of two spectra can be observed, although the peaks for the Mo/Al_2O_3 are broad and distorted. Schrader and Cheng (*23*) also obtained these two broad bands for sulfided Mo or Co–Mo/Al_2O_3 catalysts and stated that the bands arose from the distorted MoS_2 structure. Chang and Chan (*22*) reported that poorly crystalline MoS_2 shows these two sharp peaks, which can be assigned to Mo–S stretching vibration modes.

As for other supported catalysts, spectra similar to that for the Mo/Al_2O_3 were observed. Considering the above discussions, it can be assumed that MoS_2-like structures were formed on all supports after sulfurization and that the difference in the structure was more obscured for the sulfide catalysts than for the oxide catalysts. However, it should be stressed that no information on the dispersion of the catalysts was given by the spectra.

XPS. Mo $3d_{5/2}$ photoelectron spectra for calcined and sulfided catalysts are shown in Fig. 6. For the calcined catalysts, the binding energy was highly dependent on the support. Increasing binding energy has generally been considered as evidence for a higher oxidation state of the metal based on model calculations (*24, 25*). However, it should be noted that this interpretation is open to debate. Assuming a relationship between binding energy and metal oxidation state, the molybdenum species on TiO_2 were the most electronegative and those on MgO were the most electropositive. Figure 7 shows the change in Mo $3d$ spectra with increasing Mo loading on the TiO_2 support. The peak position shifted to the lower energy side with decreasing Mo loading. For the sample with 2% MoO_3 loading, Mo species with very low valence were observed. These phenomena clearly indicate that the Mo–support interaction lowered the binding energy of molybdenum. It is most probable that this low valent Mo species was produced by charge transfer from Ti^{3+} which exists in the TiO_2 support. This can account for the lower valence of Mo on TiO_2 than that on the other supports. Change in the binding energy with Mo loading has not been reported for Al_2O_3 supports (*26*).

After sulfurization, the spectra were characteristic of MoS_2 (Mo^{4+}). The full widths at half-maximum (FWHM) for all of the sulfided catalysts were smaller than those for the unsulfided catalysts (Fig. 6). This result is consistent with that of the Raman spectra. On the other hand, the spectra

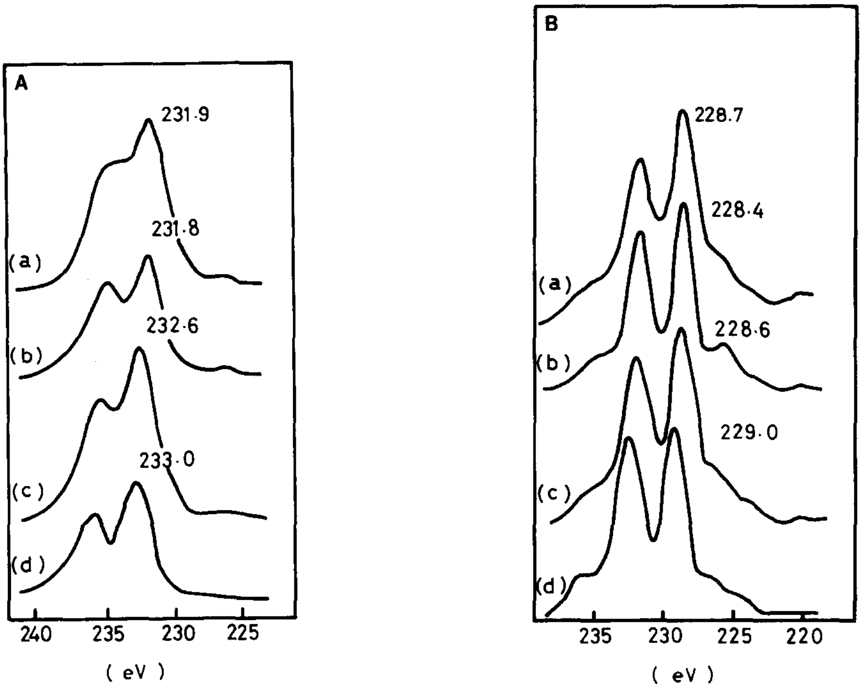

FIG. 6. Mo 3*d* photoelectron spectra for (A) oxide and (B) sulfide catalysts on various supports: (a) Mo/SiO_2, (b) Mo/TiO_2, (c) Mo/Al_2O_3, (d) Mo/MgO.

for all the catalysts clearly show the presence of Mo^{6+} species which have not been reduced to the sulfide form. This suggests that some molybdenum species bound to the support are not sulfided under the sulfiding conditions used. The presence of some unsulfided Mo^{6+} species after sulfurization implies that support effects on the catalytic properties remain to some extent on the sulfided catalyst through the residual unsulfided Mo^{6+} species. In fact, differences could be found in the electronegativity of molybdenum on each support, although they became smaller than those for oxide catalysts; Mo on TiO_2 was the most electronegative and that on MgO the most positive.

Acidity of the support and catalyst. The acid amount and acid strengths of each support or catalyst were measured using a temperature-programmed desorption (TPD) technique. NH_3 was used as the basic adsorbate. The acid amount for the supports

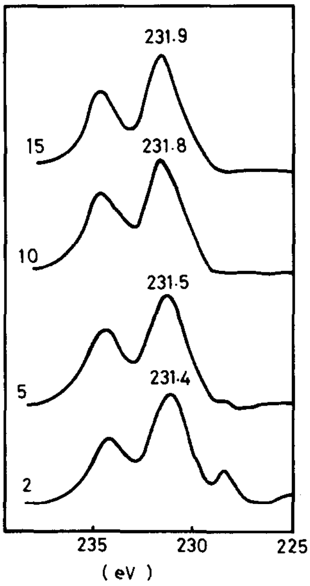

FIG. 7. Change in Mo 3*d* photoelectron spectra for Mo/TiO_2 oxide catalysts with Mo loading. (Numbers show the weight percent loading of MoO_3.)

decreased in the order of $Al_2O_3 > TiO_2 \gg SiO_2 = MgO$. The presence of molybdenum sulfide did not significantly alter the acid properties of the supports. This indicates that no acidity was introduced on the support by the active metal sulfide species. Therefore, the acid sites measured by the above method are not responsible for the HYC activity of the catalyst reported in the present study. A survey of studies on the acid properties of Mo catalysts on Al_2O_3 (*27–31*) shows that Brønsted acidity has not been observed on sulfided or reduced catalysts. There seems to be no correlation between the conventionally measured acidity and HYC activity of sulfided molybdenum catalysts.

Activities and properties of Mo catalyst. Large differences were observed in the properties or the structure of molybdate for each calcined catalyst. On the other hand, these differences became smaller after sulfiding. It is considered that support effects on the properties and structure of molybdenum species are smaller in the sulfide form than those in the oxide form. It is also inferred that the analytical techniques employed in this study do not have enough sensitivity to reveal the differences in the properties and the structures of the various sulfided catalysts. However, the effect of the support on the properties of the molybdenum catalyst will be essentially unchanged after sulfiding, because most of the strong Mo–O–support bonding will not be changed by sulfiding. Even if the bonding changes from Mo–O–support to Mo–S–support, effects of the support on the physical properties, such as dispersion or electronegativity, will remain fundamentally unchanged. From this point of view, it is important to discuss the relationship between the activity of sulfided catalysts and the properties of the oxide form from which the sulfided species come.

One of the most important catalytic properties is the dispersion of the active component on the support. The TiO_2 and Al_2O_3 supports, which showed high dispersions of molybdate, gave high HYD activity. The higher surface area of the Al_2O_3 support than that of the TiO_2 support resulted in a higher HYD activity of the former, because the TiO_2 support resulted in a lower overall active metal exposed surface area. As for SiO_2-supported catalysts, low dispersion of molybdate has been reported in previous studies (*32, 33*). In the present study, lower dispersion of molybdate on SiO_2 than that on Al_2O_3 or TiO_2 was indicated by Raman spectroscopy. One reason why SiO_2-supported catalysts gave the lowest HYD activity is their low dispersion of molybdate. Low dispersion for the SiO_2-based catalysts implies a high concentration of three-dimensional molybdate structures which are not favorable as precursors for sulfided catalyst with high HYD activity. For the MgO-supported catalyst, incorporation of molybdate into the support matrix caused a lower surface area for molybdenum than that in the Al_2O_3- or TiO_2-supported catalysts. Highly dispersed two-dimensional molybdenum species on Al_2O_3 or TiO_2 supports lead to coordinatively unsaturated molybdenum species in addition to a high surface concentration of molybdenum. Both of these properties will be favorable for increasing the number of HYD active sites on the catalyst.

As for the HYC activity of the catalysts, no correlation was found between the catalytic activity and the dispersion of molybdate. The SiO_2-supported catalyst, in spite of a lower dispersion of molybdate, showed much higher activity than the Al_2O_3-supported catalyst. Apparent correlation could not be observed between HYC activity and the acid property, either. For clarifying the effect of Brønsted acidity on the HYC of DPM, the reaction was carried out over HY zeolite. The conversion under the usual reaction conditions was extremely high, although a large amount of polymerized products was observed. It is clear that HYC of DPM is catalyzed by Brønsted acid sites on zeolites. It is possible that the HYC active sites of MoS_2 catalysts, assumed to be

Brønsted acid sites, are induced under the reaction conditions. It can be concluded that acidity measurements based on the adsorption of a basic gas, such as NH_3, do not identify the active sites for HYC. This is most likely due to the great difference in the conditions used for the acidity measurements compared to those of the HYC reactions.

Positive correlation was observed between the HYC activity and the electronegativity of molybdenum as was estimated using XPS. The TiO_2-supported catalyst with the highest HYC activity showed the most electronegative molybdenum, while the most positive molybdenum, on MgO, gave no HYC of DPM. Correlation was also found between the HYC activity and the amount of easily removable oxygen measured by the TPR method. Molybdate on the TiO_2 support was the most easily reduced, while that on the MgO was the most difficult to reduce. These results imply that electronegative molybdenum with weakly bonded oxygen is a precursor of active molybdenum sulfide species on which Brønsted acidity is induced under the reaction conditions.

One possible mechanism for the induction of Brønsted acid sites on molybdenum sulfide is by adsorption and dissociation of H_2S on sulfur vacancies (*4, 34*). In fact, hydrodenitrogenation over molybdenum sulfide catalyst was accelerated by increasing H_2S concentration in the gas phase (*35, 36*). It can be inferred that the dissociation of adsorbed H_2S occurs more easily on the electronegative molybdenum species.

Discussions on the active sites of sulfided molybdenum (or cobalt–molybdenum, nickel–molybdenum) catalysts have lead to the conclusion that there occurs, at least, two kinds of active sites on molybdenum sulfide catalysts (*2–4*). One kind of active site, which can facilitate hydrogenation and direct extrusion of sulfur, is a sulfur vacancy associated with molybdenum atoms (*2–4*). The other kind of active site is also a sulfur vacancy, on which dissociated H_2S forms a Brønsted acid site (*4*). As has been shown above, HYD of 1-MN is catalyzed on the former site, HYC of DPM on the latter one. HDS of DBT is catalyzed on both kinds of active sites; direct extrusion of sulfur proceeds on the former site, and hydrogenolysis of C–S bond is catalyzed on the latter one. Considering the reaction mechanism, it can be inferred that hydrogenated compounds are more easily produced on the "hydrogenolysis active site" than on the "direct extrusion active site." On the SiO_2-supported catalyst, hydrogenolysis exceeds direct extrusion of sulfur, leading to a high ratio of HBP/BP (Table 1).

Attention must be paid to the difference in surface concentrations of molybdenum on each support. The surface area of the Al_2O_3 support was around three times that of the TiO_2 support, the surface concentration of Mo on Al_2O_3 being one-third of that on TiO_2. The structure of molybdate on the Al_2O_3 support changes from tetrahedral to octahedral with increasing Mo loading. Hall and co-researchers (*37, 38*) reported that the amount of easily removable oxygen by TPR measurements increased with the Mo loading and that the oxygen was removed from polymolybdate that had the octahedral structure. Highly aggregated molybdate with an octahedral structure may serve as a precursor for active sulfide catalysts in HYC.

CONCLUSION

As has been shown above, significant support effects were found on the HYD and HYC activities of molybdenum sulfide catalysts. Characterization of the supported catalysts clarified the differences in the structure and properties that exist between them. It was found that two-dimensional polymolybdate structures, as determined at the stage of calcined oxide catalyst, were favorable for high HYD activity, while electronegative molybdenum which induces Brønsted acidity was required for high HYC activity.

However, the relationship between the

activities and properties of sulfide catalysts could not be clarified. It is assumed that the differences in the structure of properties among the sulfide catalysts were too small to be detected. Other characterization techniques such as EXAFS (extended X-ray absorption fine structure) are now being investigated in order to obtain more information about the properties and structure of Mo sulfide catalysts.

REFERENCES

1. Weller, S. W., *in* "Proceedings of 4th International Conference on the Chemistry and Uses in Molybdenum." Climax Molybdenum Co., Golden, CO, 1982.
2. Tanaka, K., and Okuhara, T., *Catal. Rev. Sci. Eng.* **15,** 249 (1977).
3. Massoth, F. E., and MuraliDhar, G., *in* "Proceedings of 4th International Conference on the Chemistry and Uses of Molybdenum." Climax Molybdenum Co., Golden, CO, 1982.
4. Yang, S. H., and Satterfield, C. N., *J. Catal.* **81,** 168 (1983).
5. Hattori, H., Tanabe, K., Tanaka, K., and Okazaki, S., *in* "Proceedings of 3rd International Conference on the Chemistry and Uses of Molybdenum." Climax Molybdenum Co., Ann Arbor, MI, 1979.
6. Swanson, W. W., Streusand, B. J., and Tsigdinos, G.A., *in* "Proceedings of 4th International Conference on the Chemistry and Uses of Molybdenum." Climax Molybdenum Co., Golden, CO, 1982.
7. MuraliDhar, G., Massoth, F. E., and Shabtai, J., *J. Catal.* **85,** 44 (1984).
8. Massoth, F. E., MuraliDhar, G. and Shabtai, J., *J. Catal.* **85,** 53 (1984).
9. Shimada, H., Kurita, M., Sato, T., Yoshimira, Y., Hirata, T., Konakahara, T., Sato, K., and Nishijima, A., *Chem. Lett.,* 1861 (1984).
10. Nishijima, A., Shimada, H., Sato, T., Yoshimura, Y., and Hiraishi, J., *Polyhedron* **5,** 243 (1986).
11. Nishijima, A., Shimada, H., Sato, T., and Yoshimura, Y., *in* "Proceedings of 1985 International Conference on Coal Science, Sydney, Australia."
12. Tanabe, K., "Solid Acids and Bases." Academic Press, New York, 1970.
13. Brown, F. R., Makovsky, L. E., and Rhee, K. H., *J. Catal.* **50,** 162 (1977).
14. Cheng, C. P., and Schrader, G. L., *J. Catal.* **60,** 276 (1979).
15. Jeziorowski, H., and Knozinger, H., *J. Phys. Chem.* **83,** 1166 (1979).
16. Sombret, B., Dhamelincourt, P., Wallart, F., Muller, A. C., Bouquet, M., and Grosmangin, J., *J. Raman Spectrosc.* **9,** 291 (1980).
17. Thomas, R., van Oers, E. M., de Beer, V. H. J., Medema, J., and Moulijin, J. A., *J. Catal.* **76,** 241 (1982).
18. Wang, L., and Hall, W. K., *J. Catal.* **66,** 251 (1980).
19. Dufresne, P., Payen, E., Grimblot, J., and Bonnelle, *J. Phys. Chem.* **85,** 2344 (1981).
20. Sonnemans, J., and Mars, P., *J. Catal.* **31,** 209 (1973).
21. Ng, K. Y. S., and Gulari, E., *J. Catal.* **92,** 340 (1985).
22. Chang, C. H., and Chan, S. S., *J. Catal.* **72,** 139 (1981).
23. Schrader, G. L., and Cheng, C. P., *J. Catal.* **85,** 488 (1984).
24. Siegbahn, K., Nordling, C., Fahlman, A., Nordberg, B., Hamrin, K., Hedman, J., Johansson, G., Bergmark, T., Karlsson, S. E., Lindgren, I., and Lindberg, B., "ESCA Atomic, Molecular and Solid State Structure Studied by Means of Electron Spectroscopy." Nova Acta Regiae Soc. Sci. Upsaliensis, Ser. 20, Almqvist & Wiksells Boktryekeri AB, Stockholm, 1967.
25. Fadley, C. S., Hagstrom, S. B. M., Klein, M. P., and Shirley, D. A., *J. Chem. Phys.* **48,** 3779 (1968).
26. Zingg, D. S., Makovsky, L. E., Tischer, R. E., Brown, F. R., and Hercules, D. M., *J. Phys. Chem.* **84,** 2898 (1980).
27. Kiviat, F. E., and Petrakis, L., *J. Phys. Chem.* **77,** 1232 (1972).
28. Mone, R., *in* "Preparation of Catalysts" (B. Delmon, P. A. Jacobs, and G. Poncelet, Eds.), p. 381. Elsevier, Amsterdam, 1976.
29. Ratnasamy, R., and Knozinger, H., *J. Catal.* **54,** 155 (1978).
30. Riseman, S. M., Bandyopadhyay, S., Massoth, F. E., and Eyring, E. M., *Appl. Catal.* **16,** 29 (1985).
31. Boorman, P. M., Kydd, R. A., Sarbak, Z., and Somogyvari, A., *J. Catal.* **100,** 287 (1986).
32. MuraliDhar, G., Concha, B. E., Bartholomew, G. L., and Bartholomew, C. H., *J. Catal.* **89,** 274 (1984).
33. Cid, R., Villasenor, J., Orellana, F., Fierro, J. L. G., and Lopez Agudo, A., *Appl. Catal.* **18,** 357 (1985).
34. Yang, S. H., and Satterfield, C. N., *Ind. Eng. Chem. Process Des. Dev.* **81,** 168 (1983).
35. Satterfield, C. N., and Gultekin, S., *Ind. Eng. Chem. Process Des. Dev.* **20,** 62 (1981).
36. Inoue, Y., *in* "Proceedings of 1985 International Conference on Coal Science, Sydney, Australia."
37. Hall, W. K., and Massoth, F. E., *J. Catal.* **34,** 41 (1974).
38. Hall, W. K., *in* "Proceedings of 4th International Conference on the Chemistry and Uses of Molybdenum. "Climax Molybdenum Co., Golden, CO, 1982.